

## On the Reactivity of $\text{Ti}^+(\text{}^4\text{F}, \text{}^2\text{F})$ . Reaction of $\text{Ti}^+$ with $\text{OH}_2$

Arantxa Irigoras, Joseph E. Fowler, and Jesus M. Ugalde\*

Kimika Fakultatea, Euskal Herriko Unibertsitatea, P.K. 1072, 20080 Donostia, Euskadi, Spain

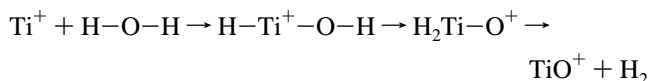
Received: September 29, 1997<sup>®</sup>

The reaction of  $\text{Ti}^+(\text{}^4\text{F}, \text{}^2\text{F}) + \text{OH}_2$  has been studied in detail for both doublet and quartet spin states. The only exothermic products are  $\text{TiO}^+(\text{}^2\Delta)$  and  $\text{H}_2$ ; formation of several endothermic products is also examined. An in-depth analysis of the reaction paths leading to each of the observed products is given, including various singlet, triplet, and quartet minima, several important transition states, and a discussion of the two  $\text{H}_2$  elimination mechanisms proposed in the literature. The experimentally observed spin-forbidden crossing is given a possible explanation. Throughout this work comparison to experimental results in energetics, reaction products, and suggested mechanisms has been central.

### 1. Introduction

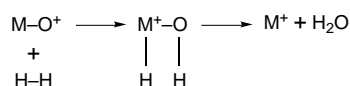
Transition metal cation chemistry has been the subject of many experimental studies in recent years. At the same time, theoretical studies have seen a rapid increase in applicability thanks to improved computational methods and new computational technologies.<sup>1</sup> These developments in both the experimental and theoretical fields provide new opportunities to study quantitatively the reactions, mechanisms, bonding, and structure of complexes incorporating transition metals.<sup>2,3</sup>

Of particular interest among recent works, e.g., refs 4–9, are the results presented by Castleman and co-workers<sup>10</sup> indicating that  $\text{Ti}^+$  is very active toward breaking C–H, O–H, N–H, and C–O bonds in small alkene molecules, ammonia, water, and methanol. All the reactions are exothermic bimolecular reactions at thermal energies. For these reactions, the dehydrogenation rate constant is found to be proportional to the bond strength of the X–H bonds. The result can be explained on the basis of dehydrogenation mechanisms. For example:



Here, a H migration from O to Ti occurs in the mechanism, following the initial insertion of  $\text{Ti}^+$  into the O–H bond.

More recently Armentrout and co-workers<sup>11</sup> have found, after an exhaustive experimental study, that the early transition metal ions ( $\text{Sc}^+$ ,  $\text{Ti}^+$ , and  $\text{V}^+$ ) are more reactive than their oxides, while the contrary occurs with the late metals ( $\text{Cr}^+$ ,  $\text{Mn}^+$ , and  $\text{Fe}^+$ ). The energetics measured for these reactions correspond to production of  $\text{M}^+$  primarily in an excited low-spin electronic state; formation of ground-state  $\text{M}^+$  is also observed, even though this reaction channel does not conserve spin. Their proposed mechanism that appears to be consistent with all their experimental and molecular orbital considerations is



where the intermediate  $\text{HM}^+\text{OH}$  moiety conserves spin with

the  $\text{MO}^+ + \text{H}_2$  reactants and the low-spin  $\text{M}^+ + \text{H}_2\text{O}$  products, but not the ground-state  $\text{M}^+ + \text{H}_2\text{O}$  products.

Their data for the titanium and vanadium systems are dominated by production of excited low-spin  $\text{Ti}^+(\text{}^2\text{F})$  and  $\text{V}^+(\text{}^3\text{F})$  states. Their estimated potential energy surface, on the basis of their results and theoretical predictions of Tilson and Harrison,<sup>12</sup> shows for  $\text{Sc}^+$  a crossing of the triplet and singlet surfaces, probably occurring in the region between  $\text{HSc}^+\text{OH}$  and  $\text{Sc}(\text{OH}_2)^+$ . Similar crossing should also exist in the titanium and vanadium systems, and thus the inefficiency of forming the ground-state metal ions in these systems can be explained by the need to undergo a spin-forbidden surface crossing. The  $\text{MO}^+ + \text{D}_2 \rightarrow \text{M}^+ + \text{D}_2\text{O}$  reaction channel is the first bimolecular, transition metal reaction to their knowledge that shows convincing evidence that excited-state products can be formed preferentially over ground-state products. The overriding constraint in these systems is conservation of spin rather than overall reaction energetics.<sup>11</sup>

Finally Armentrout and co-workers<sup>13</sup> studied the reverse of the above mentioned reactions. They found that the  $\text{a}^2\text{F}$  state of  $\text{Ti}^+$  reacts much more efficiently than the  $\text{a}^4\text{F}$  ground state in forming the  $\text{MD}^+$ ,  $\text{MO}^+$ , and  $\text{MOD}^+$  product ions. All evidence is consistent with the hypothesis that the reactions occur primarily through a low-spin state of a  $\text{DM}^+\text{OD}$  intermediate. Furthermore, they suggest that this species is likely to eliminate  $\text{H}_2$  through a four-centered transition state. This is in contrast with the mechanism proposed by Castleman and co-workers,<sup>10</sup> in which the initial step of  $\text{Ti}^+$  insertion into the O–H bond to form  $\text{HTi}^+\text{OH}$  is followed by hydrogen migration to form  $\text{H}_2\text{TiO}^+$ , which then loses  $\text{H}_2$  to form  $\text{TiO}^+$ .

The data provided and questions raised by these experimental works provide an excellent point of departure for theoretical investigation. Preliminary work has been done in our group determining the dissociation energies of the  $\text{Ti}(\text{OH}_2)^+$  ion–molecule complex comparing MCSCF, CCSD(T), and DFT methods.<sup>14</sup> This present work is the first theoretical investigation of the possible mechanisms of bond activation and dissociation involved in the  $\text{Ti}(\text{OH}_2)^+$  system. We report full reaction mechanism geometries and energetics for both the doublet and quartet spin states for numerous possible reactions of  $\text{Ti}^+$  with  $\text{H}_2\text{O}$ .

<sup>®</sup> Abstract published in *Advance ACS Abstracts*, December 1, 1997.

**TABLE 1: Active Spaces Used for Multireference Calculations**

system	orbitals included	size <sup>a</sup>
Ti <sup>+</sup>	b <sub>1</sub> (d <sub>xz</sub> )b <sub>2</sub> (d <sub>yz</sub> )a <sub>2</sub> (d <sub>xy</sub> )a <sub>1</sub> (d <sub>xx-yy</sub> )a <sub>1</sub> (d <sub>2z<sup>2</sup>-xx-yy</sub> )a <sub>1</sub> (s)	(3/6)
H <sub>2</sub> O	σ(O-H, bond)r * (O-H, antibond)	(4/4)
TiOH <sup>+</sup> <sub>2</sub>	σ(O-H, bond)r * (O-H, antibond)	(4/4) + Ti <sup>+</sup> (3/6)
TiO <sup>+</sup> ( <sup>4</sup> B <sub>1</sub> )	(Ti-O, bond)(Ti-O, antibond)8a <sub>1</sub> 9a <sub>1</sub> 4b <sub>1</sub> 3b <sub>2</sub> 4b <sub>2</sub> 1a <sub>2</sub>	(7/10)
TiO <sup>+</sup> ( <sup>2</sup> A <sub>2</sub> )	2(Ti-O, bond)2(Ti-O, antibond)8a <sub>1</sub> 9a <sub>1</sub> 4b <sub>1</sub> 1a <sub>2</sub>	(5/8)
H <sub>2</sub>	σ <sub>g</sub> σ <sub>u</sub> <sup>*</sup>	(2/2)
TiOH <sup>+</sup>	(Ti-O, bond)(O-H, bond)(Ti-O, antibond)(O-H, antibond)4a''5a''10a'11a'	(6/9)
HTiO <sup>+</sup>	2(Ti-O, bond)(Ti-H, bond)2(Ti-O, antibond)(Ti-H, antibond)4a''5a''10a'	(6/9)

<sup>a</sup> The notation (*m/n*) denotes an active space of *m* electrons in *n* orbitals.

**TABLE 2: Total Energies (*E*), in hartree, Zero-Point Vibrational Energy Corrections ( $\Delta$ ZPVE), Basis Set Superposition Error Corrections (BSSE), and Dissociation Energies (*D*<sub>0</sub>) in eV, for the Ti(OH<sub>2</sub>)<sup>+</sup> Ion–Molecule Complex**

method <sup>a</sup>		<i>E</i>	$\Delta$ ZPVE	BSSE	<i>D</i> <sub>0</sub>
B3LYP	DZVP	-925.511 90	0.078	0.039	1.619
	LanL2DZ	-134.224 60	0.078	0.148	1.684
	TZVP+G(3df,2p)	-925.649 49	0.074	0.022	1.573
CASPT2(7/10)[11]	Wachters	-924.516 53	0.069	0.178	1.536
CASPT2(7/10)[6]	Wachters	-924.732 65	0.069	0.221	1.654
CASPT2(7/10)[0]	Wachters	-924.749 28	0.069	0.230	1.654
experimental <sup>6</sup>					1.65 ± 0.13
experimental <sup>4</sup>					1.60 ± 0.06
theoretical <sup>36</sup>					1.626

<sup>a</sup> For the CASPT2 results, the numbers in parentheses (*m/n*) incideate the size of the active space (*m* electrons in *n* orbitals), and in square brackets are the number of frozen core orbitals.

## 2. Methods

The computational method used for optimization and frequency calculations was density functional theory (B3LYP functional)<sup>15,16</sup> with the DZVP basis sets given by Salahub et al.<sup>17,18</sup> because of the good results obtained in previous works.<sup>14</sup> The choice of the B3LYP DFT method is largely motivated by its satisfactory performance reported recently<sup>1,19,20</sup> for transition metal containing systems. Some of the more relevant structures have been reoptimized at the B3LYP/LanL2DZ level to see how the triple- $\zeta$  treatment of the 3d electrons influences geometries and energies. Reactants and products of the possible reactions have been reoptimized at both the B3LYP/6-311+G(2d,2p) and B3LYP/TZVP+G(3df,2p) levels for the system. All the calculations have been corrected with the ZPVE calculated at the corresponding theoretical level. The triple- $\zeta$  quality basis set, TZVP+G(3df,2p), used for titanium was that given by Schäfer, Hubert, and Ahlrichs,<sup>21</sup> supplemented with a diffuse s function (with an exponent 0.33 times that of the most diffuse s function on the original set), two sets of p functions optimized by Wachters<sup>22</sup> for the excited states, one set of diffuse pure angular momentum d function (optimized by Hay),<sup>23</sup> and three sets of uncontracted pure angular momentum f functions, including both tight and diffuse exponents, as recommended by Ragavachari and Trucks.<sup>24</sup> For the oxygen and hydrogen atoms, the 6-311++G(2df,2p) basis set of Pople et al.<sup>25</sup> was used.

In order to give very accurate energies for the energy differences between the different spin states of each species, CASPT2 calculations have been carried out.<sup>26,27</sup> In the CASPT2 calculations the Wachters primitive basis for titanium<sup>22</sup> was extended by adding two sets of p functions in the 4p region, one 5d set of diffuse d functions, and three 7f sets of f functions, yielding a (14s,11p, 6d, 3f) primitive basis. This was contracted to a [6s, 5p, 3d, 1f] basis as explained in ref 28. For oxygen the primitive (9s, 5p) basis of Huzinaga<sup>29</sup> was used, contracted to [3s, 2p] plus one set of pure angular momentum d functions. For hydrogen the primitive (5s) augmented with one set of p functions and contracted to [3s, 1p] was used. The active spaces used for the CASPT2 calculations are given in Table 1. The

criterion used to choose this active spaces is the “chemically reasonable” one.<sup>30</sup> That is, all MOs taking part in forming and breaking bonds were included in the active space.

All DFT calculations reported in this paper have been carried out with the GAUSSIAN94/DFT<sup>31</sup> suites of programs, and the CASPT2 calculations were carried out with the MOLCAS program.<sup>32</sup> Also NBO<sup>33,34</sup> calculations have been done to clarify some structures, and MOLDEN<sup>35</sup> was used to draw MO pictures.

## 3. Results and Discussion

Our discussion will focus first on the Ti(OH<sub>2</sub>)<sup>+</sup> dissociation energy and then the quartet  $\rightarrow$  doublet splitting for several relevant species. Following these are total energies for the experimentally observed reactions, and this report finishes with a detailed analysis of the PES.

**3.1. Ti(OH<sub>2</sub>)<sup>+</sup> Dissociation Energy.** Dissociation energies of the Ti(OH<sub>2</sub>)<sup>+</sup> ion–molecule have been calculated with new levels of theory and compared with the ones calculated in a previous work by this group<sup>14</sup> in order to test the quality of these methods in describing these reactions. Dissociation energies were calculated as the difference between the energy of the isolated monomers and the complex, including both BSSE and ZPVE corrections.

Ti(OH<sub>2</sub>)<sup>+</sup> dissociation energies predicted by various levels of theory<sup>36</sup> and those experimentally observed<sup>4,6</sup> are given in Table 2. The  $\Delta$ ZPVE values for the multireference methods were taken as the average of all other results reported for this system.<sup>14</sup> It can be seen that a slightly higher *D*<sub>0</sub> is predicted for the B3LYP/LanL2DZ than for the B3LYP/DZVP theory level, although the results obtained with Los Alamos effective core potentials are similar to the ones obtained previously with the SKBJC effective core potentials.<sup>14</sup>

The predictions of the CASPT2 method demonstrate the importance of properly including dynamic/nondynamic correlation in order to obtain a good description of the system. When the 1s through 3p orbitals of the titanium and the 1s orbital of oxygen are not correlated (10 frozen core orbitals), the dis-

sociation energy obtained is clearly underestimated. This shortcoming is quickly resolved through reducing the frozen core to include only the 1s2s2p orbitals of Ti and the 1s orbital of O. Further reduction of the frozen core does not change the predicted dissociation energy.

**3.2. Excitation Energy.** In the reactions of interest there are three quartet–doublet relative energies that are exceptionally important; thus, we describe them more exhaustively. These three are the Ti<sup>+</sup>, Ti(OH<sub>2</sub>)<sup>+</sup>, and TiO<sup>+</sup> moieties. Excitation energies for these systems are shown in Table 3.

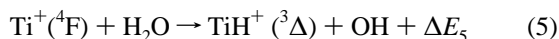
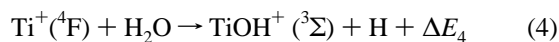
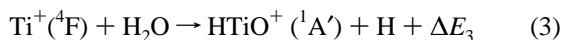
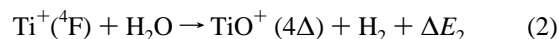
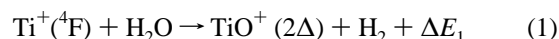
It is known that DFT calculations can describe properly ground states even for transition metal systems and also that this method gives good results for some excited-state calculations.<sup>1,19,20</sup> For the Ti<sup>+</sup> system, for example, the doublet state is a three-electron doublet state, which can be formed through various orbital occupations. Thus it is difficult to describe properly with single-determinant methods. However, the results obtained with the B3LYP method are reasonably close to other theoretical predictions as well as experimental observations.

The CASPT2 calculation results are even closer in agreement with the experimental value for the Ti<sup>+</sup> <sup>4</sup>F → <sup>2</sup>F excitation energy. Note that again when the 1s–3p orbitals of Ti are frozen an underestimation of the energy is observed, but the results obtained from the freezing of the 1s through 2p orbitals are equivalent with the nonfrozen core results.

Quartet → doublet excitation energies for the Ti(OH<sub>2</sub>)<sup>+</sup> ion–molecule also have been calculated at numerous levels of theory. Armentrout and co-workers<sup>13</sup> assumed this energy difference to be the same as for the Ti<sup>+</sup> cation. At the B3LYP level, with both basis sets used, the energy difference found is lower than the predicted Ti<sup>+</sup> <sup>4</sup>F → <sup>2</sup>F energy gap. However, this energy difference predicted by the various CASPT2 levels is approximately twice that predicted by the B3LYP method.

The last system studied at these levels was the TiO<sup>+</sup> molecule. Here the doublet is the ground state. Armentrout and co-workers<sup>13</sup> estimated that the high-spin states of TiO<sup>+</sup> lie above the low-spin ground state by about 3.5 eV. The CASPT2 predictions are in good agreement with their estimations, and the B3LYP numbers are only slightly lower.

**3.3. Reaction Energetics.** Five reactions leading to the experimentally observed product ions have been studied for this system:



Equations 1–5 represent the main ionic products observed in the reaction of Ti<sup>+</sup>(<sup>4</sup>F) and H<sub>2</sub>O. The energetics of these reactions have been calculated with the B3LYP and CASPT2 methods, and here larger basis sets also have been used with the B3LYP method. The various predicted values and the energies given by Armentrout and co-workers<sup>13</sup> are listed in Table 4.

In some of these energetics, we see very large discrepancies between the B3LYP predictions resulting from the use of different basis sets. In each case the difference between the B3LYP/DZVP result and the B3LYP/LanL2DZ result is star-

**TABLE 3: Relative Energies in eV for the <sup>4</sup>F(sd<sup>2</sup>) and <sup>2</sup>F(sd<sup>2</sup>) States of Ti<sup>+</sup> (Δ<sub>1</sub>), the <sup>4</sup>B<sub>1</sub> and <sup>2</sup>B<sub>2</sub> States of Ti(OH<sub>2</sub>)<sup>+</sup> (Δ<sub>2</sub>), and the <sup>4</sup>Δ and the <sup>2</sup>Δ States of TiO<sup>+</sup> (Δ<sub>3</sub>)**

method <sup>b</sup>	Δ <sub>1</sub>	Δ <sub>2</sub>	Δ <sub>3</sub>
B3LYP/DZVP	0.599	0.593	−3.045
B3LYP/LanL2DZ	0.647	0.510	−2.991
B3LYP/TZVP+G(3df,2p)	0.545	0.488	−3.111
CASPT2[9,10]/Wachters	0.507	0.850	−3.450
CASPT2[5,6]/Wachters	0.596	1.023	−3.517
CASPT2[0,0]/Wachters	0.597	1.117	−3.524
experimental <sup>3,38</sup>	0.574	0.565 <sup>a</sup>	−3.5 <sup>a</sup>

<sup>a</sup> Estimated. <sup>b</sup> In square brackets the total number of frozen orbitals are shown; the first number corresponds to the Ti<sup>+</sup>, and the second one to Ti(OH<sub>2</sub>)<sup>+</sup> and TiO<sup>+</sup> moieties. The CAS active space used for each calculation can be found in Table 1.

ting. However, some consistency is seen with the larger 6-311+G(2d,2p) and TZVP+G(3df,2p) basis sets. This consistency and the reasonable agreement with experimental<sup>13</sup> results implies that the B3LYP/TZVP+G(3df,2p) level of theory provides results worthy of a high level of confidence.

In agreement with experiment, we find only one exothermic reaction, the formation of low-spin TiO<sup>+</sup>+H<sub>2</sub> (reaction 1). Our best value of 1.543 eV is 0.23 eV below the experimentally observed energy. Considering that a spin-crossing is involved in this reaction, our energy predictions are good, but not entirely satisfactory. The result, −0.321 eV, obtained for the low-lying endothermic reaction leading to TiOH<sup>+</sup>+H, Reaction 4, is within the error bars of the experimental result, −0.39 ± 0.12 eV. The experimental value for reaction 2 (−1.73 eV) is based on an estimated doublet → quartet splitting of 3.5 eV<sup>13</sup> and is not radically different from our calculated −1.568 eV.

**3.4. The Doublet Stationary Points.** The various B3LYP/DZVP doublet stationary points are depicted in Figure 1. The C<sub>2v</sub> symmetry Ti(OH<sub>2</sub>)<sup>+</sup> ion–molecule complex has a Ti–O distance of 2.104 Å and a Ti–O stretching frequency of 401 cm<sup>−1</sup>. As seen in the dissociation energies section, this interaction is rather strong. However, the OH<sub>2</sub> moiety itself is only slightly changed from its unassociated parameters. In comparison to free H<sub>2</sub>O described by the same level of theory, the O–H bond length in this complex is 0.008 Å longer and the symmetric stretching and H–O–H bending frequencies change by −93 and 21 cm<sup>−1</sup> respectively.

TS1 characterizes the first hydrogen transfer from oxygen to titanium. This transition state has C<sub>s</sub> symmetry, and the one imaginary frequency clearly corresponds to hydrogen transfer.

The HTi<sup>+</sup>OH minimum also has C<sub>s</sub> symmetry. This intermediate is a well-characterized minimum with a covalent Ti–H bond. The Ti–H stretching frequency is 897 cm<sup>−1</sup>, and the H–Ti–O bend has a frequency of 482 cm<sup>−1</sup>. The lowest vibrational frequency of 281 cm<sup>−1</sup> corresponds to the Ti–O–H bend.

The second oxygen to titanium hydrogen transfer occurs through TS2. In this transition state the H–H distance is still quite long (0.983 Å) and the Ti–O distance (1.691 Å) is closer to the HTiOH value than that in the following (H<sub>2</sub>)TiO species. The one imaginary frequency corresponds to H–H bond formation.

The final doublet stationary point located was the (H<sub>2</sub>)TiO<sup>+</sup> species. This (H<sub>2</sub>)TiO<sup>+</sup> structure of C<sub>s</sub> symmetry is a curious intermediate. Earlier arguments against H<sub>2</sub> elimination from an H<sub>2</sub>TiO<sup>+</sup> structure have considered two covalent Ti–H bonds.<sup>10</sup> The (H<sub>2</sub>)TiO<sup>+</sup> minimum that exists on the PES has no Ti–H σ bonds per se, but should be considered a ion–molecule complex. Note that the Ti–H bond distance has increased from 1.656 Å in the HTi<sup>+</sup>OH minimum to 2.115 Å

**TABLE 4: Overall Energies for Reactions 1–5 at Several Levels of Theory<sup>a</sup>**

method	$\Delta E_1$	$\Delta E_2$	$\Delta E_3$	$\Delta E_4$	$\Delta E_5$
B3LYP/DZVP	1.365	-1.680	-1.661	-0.470	-2.739
B3LYP/LanL2DZ	1.642	-1.349	-1.470	-0.200	
B3LYP/6-311+G(2d,2p)	1.536	-1.573	-1.306	-0.341	
B3LYP/TZVP+G(3df,2p)	1.543	-1.568	-1.293	-0.321	-2.632
CASPT2[9,10]	1.308	-2.142	-1.572	-0.676	
CASPT2[5,6]	1.314	-2.203	-1.434	-0.669	
CASPT2[0]	1.315	-2.209	-1.420	-0.664	
experimental <sup>13</sup>	1.77 ± 0.06	-1.73 <sup>b</sup>		-3.9 ± 0.12	-2.74 ± 0.09

<sup>a</sup> Energies given are in eV, and for the various B3LYP levels of theory include ZPVE corrections calculated at the corresponding level of theory.  
<sup>b</sup> Estimated.

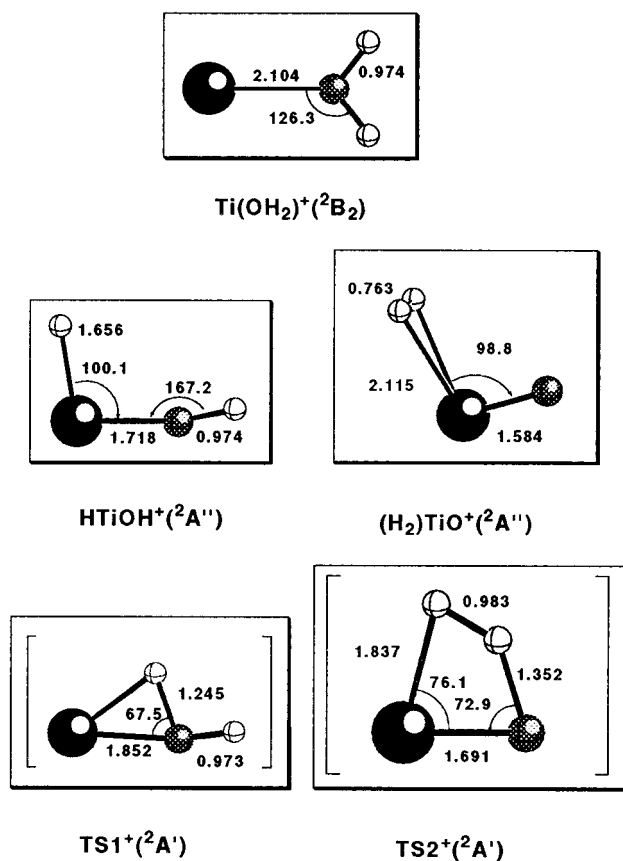


**Figure 1.** Geometrical parameters of the various stationary points on the doublet B3LYP/DZVP potential energy surface. Bond lengths are reported in Å, bond angles in deg.

here. Examination of the MOs shows an interaction between the singly occupied d orbital of Ti and the H–H  $\sigma^*$  orbital (see Figure 2). NBO analysis gives this interaction a value of 7.87 kcal/mol. It is through this interaction that the H–H bond is activated. In comparison with separated  $\text{TiO}^+(\text{}^2\Delta) + \text{H}_2$ , the Ti–O bond length of this complex is only 0.004 Å longer, while the aforementioned H–H bond activation lengthens the H<sub>2</sub> bond length by 0.02 Å.

**3.5. Quartet Stationary Points.** Figure 3 depicts the various B3LYP/DZVP quartet stationary points. The stationary points found on the quartet surface are in many aspects related to those of the doublet surface. The  $\text{Ti(OH}_2\text{)}^+$  ion–molecule is very similar indeed. The geometrical parameters of both are essentially equal and the vibrational frequencies which that the greatest are the water wagging frequency, which decreases here by 52  $\text{cm}^{-1}$ , and the Ti–O stretching frequency, which increases by 57  $\text{cm}^{-1}$ .

The HTi<sup>+</sup>OH species, on the other hand, is quite different on the quartet surface. The Ti–O bond is 0.048 Å longer for

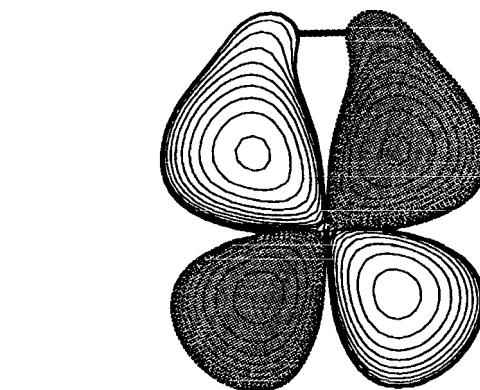


**Figure 2.** Singly occupied orbital of the doublet  $(\text{H}_2)\text{TiO}^+$  intermediate as seen looking down the Ti–O axis.

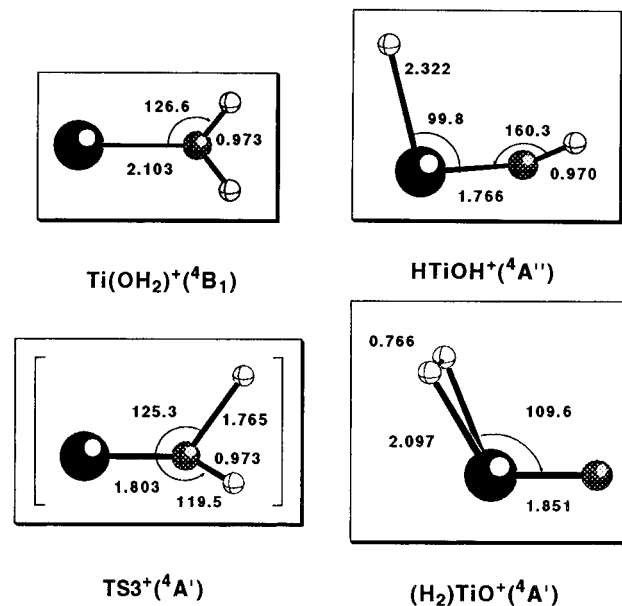


**Figure 3.** Geometrical parameters of the various stationary points on the quartet B3LYP/DZVP potential energy surface. Bond lengths are reported in Å, bond angles in deg.

the quartet minimum, and the Ti–H bond an astounding 0.666 Å longer. This difference is also seen in the Ti–O and Ti–H stretching frequencies, which are 101 and 1287  $\text{cm}^{-1}$  lower for the quartet than the doublet species.

The  $(\text{H}_2)\text{TiO}^+$  ion–molecule complex on the quartet surface has a slightly stronger interaction between the H<sub>2</sub> molecule and the  $\text{TiO}^+$  unit than that found on the doublet surface. However, as was the case on the doublet surface, this structure should not be considered to have two covalent Ti–H bonds, but rather a  $d \rightarrow \sigma^*$  donation. For the quartet species, this interaction is given a value of 9.85 kcal/mol by NBO analysis.

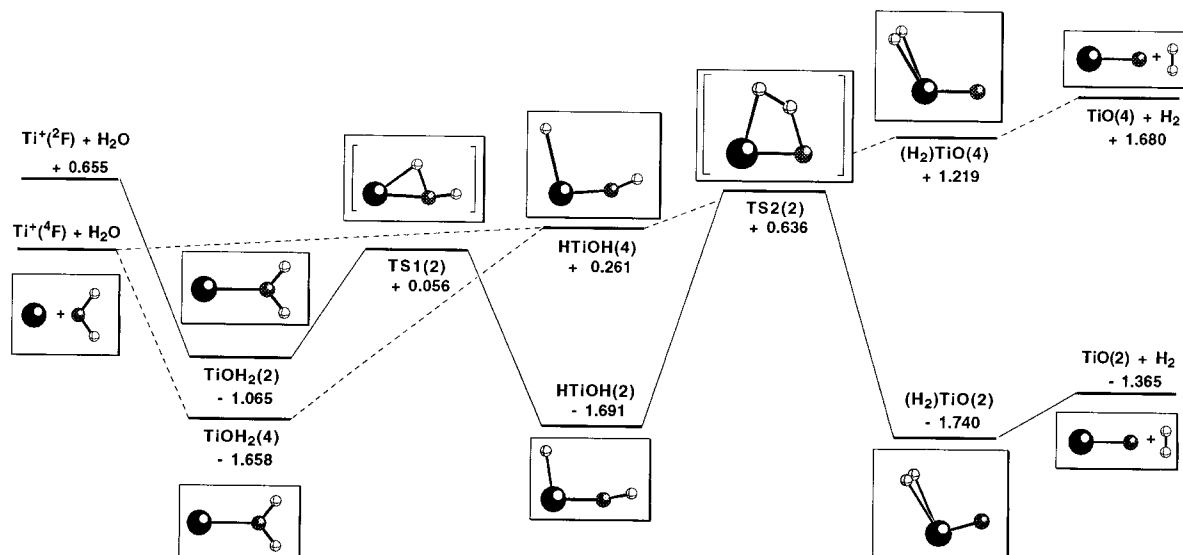


**Figure 4.** B3LYP/DZVP potential energy surface following the  $\text{Ti}^+ + \text{OH}_2 \rightarrow \text{TiO}^+ + \text{H}_2$  reaction path. Energies given are in eV and relative to the separated ground-state reactants,  $\text{Ti}^+(^4\text{F}) + \text{OH}_2$ . Bond lengths are reported in Å, bond angles in deg.

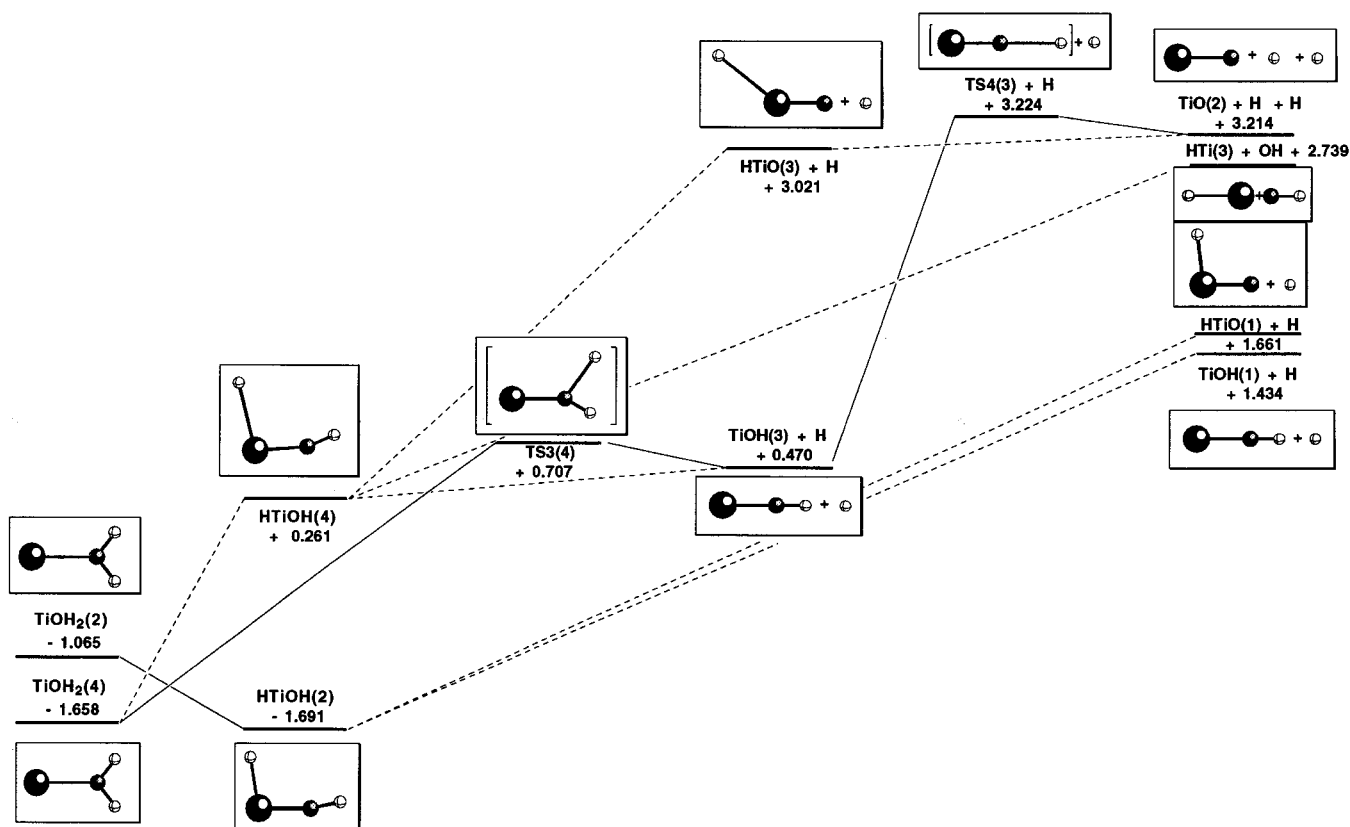


**Figure 5.** B3LYP/DZVP potential energy surface following the reaction paths leading to the other experimentally observed products. Energies given are in eV and relative to the separated ground-state reactants,  $\text{Ti}^+(^4\text{F}) + \text{OH}_2$ . Bond lengths are reported in Å, bond angles in deg.

**3.6. Potential Energy Surfaces.** Figure 4 shows the potential energy surface starting from the  $\text{Ti}^+ + \text{OH}_2$  separated reactants and leading to  $\text{TiO}^+ + \text{H}_2$  for the doublet and quartet spin states at the B3LYP/DZVP level of theory.

On the doublet surface, the first step is the formation of the ion–molecule complex. Then, through TS1, one hydrogen atom is passed from oxygen to titanium, leading to the  $\text{HTi}^+\text{OH}$  molecule, the intermediate whose existence was surmised by experimentalists.

A second hydrogen transfer from oxygen to titanium passing through TS2 leads to the most stable complex encountered on

the surface,  $(\text{H}_2)\text{TiO}^+$ . From this intermediate the loss of  $\text{H}_2$  proceeds without transition state to the observed major products, doublet  $\text{TiO}^+$  and  $\text{H}_2$ .

The first step on the quartet surface can also be formation of the ion–molecule complex. However, following the reaction from that point is significantly more complicated than was the case for the doublet surface. Despite numerous varied strategies for finding a transition state between this complex and the  $\text{HTi}^+\text{OH}$  molecule, none was found. Here we note that while the quartet  $\text{Ti}(\text{OH}_2)^+$  ion–molecule complex lies below that of the doublet, their relative positions are reversed in the  $\text{HTi}^+\text{OH}$

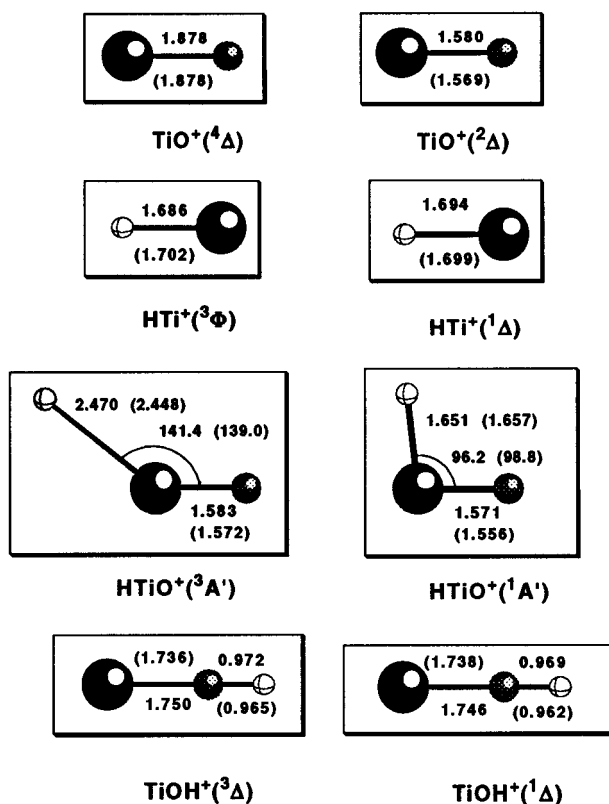


**Figure 6.** Equilibrium geometry parameters for the various reaction products at the B3LYP/DZVP level of theory. In parentheses are the parameters predicted at the B3LYP/TZ+G(3df,2p) level of theory. Bond lengths are reported in Å, bond angles in deg.

moieties. Thus, the two surfaces have crossed somewhere between these two points. This explains the experimentally observed “forbidden crossing” and seriously complicates the location of the quartet transition state.

Once this quartet  $\text{HTi}^+\text{OH}$  intermediate is formed possibly from  $\text{Ti}(\text{OH}_2)^+$  rearrangement, possibly from direct  $\text{Ti}^+$  insertion into an O–H bond of  $\text{H}_2\text{O}$ , another intermediate,  $(\text{H}_2)\text{TiO}^+$ , can be realized by passing through another probably high-lying H transfer transition state. From that isomer, the loss of an  $\text{H}_2$  molecule gives one of the scarcely observed reaction products, quartet  $\text{TiO}^+$ . The high relative energy of this product agrees well with the fact that  $\text{TiO}^+$  in this spin state is a rarely observed reaction product.

Figure 5 depicts the doublet and quartet B3LYP/DZVP potential energy surfaces for the reactions leading to the other experimentally observed products,  $\text{TiOH}^+$  and  $\text{TiH}^+$ , sequential H atom loss leading to  $\text{TiO}^+$ , and the possible reactions leading to  $\text{HTiO}^+$  and  $\text{TiH}^+ + \text{OH}$ . Energies given (in eV) are relative to  $\text{Ti}(^4\text{F}) + \text{H}_2\text{O}$  (as was the case in Figure 4).

The doublet process begins with the formation of the  $\text{Ti}(\text{OH}_2)^+$  ion–molecule and passes through the H atom transfer transition state, resulting in the  $\text{HTi}^+\text{OH}$  intermediate. This doublet  $\text{HTi}^+\text{OH}$  may lose one of its hydrogen atoms, leading to either the singlet  $\text{HTiO}^+$  or  $\text{TiOH}^+$ . These two species are relatively close in energy, but as would be expected, the  $\text{TiOH}^+$  isomer is lower in energy. Note that the energy difference between these two singlet isomers is much smaller than the energy difference between the corresponding triplet isomers.

The quartet surface is, again, more complicated than that of the doublet. Considering the  $\text{Ti}(\text{OH}_2)^+$  ion–molecule complex, it is possible (passing through TS3) that one H atom is directly lost from the oxygen, leading to the triplet  $\text{TiOH}^+$  species. This

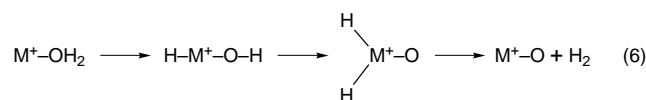
molecule also could lose its remaining hydrogen atom through TS4. This pathway leads to eventual formation of doublet  $\text{TiO}^+$  but is very much kinetically disfavored as compared to the pathway in Figure 2 because it passes through a very high-lying transition state (TS4).

Considering the quartet  $\text{HTi}^+\text{OH}$  species, it is possible that either of the two H atoms could be lost individually, resulting in the triplet  $\text{TiOH}^+$  or high-lying  $\text{HTiO}^+$  triplet. Again, there is the possibility of forming the doublet  $\text{TiO}^+$  product from either of these minima through loss of the second hydrogen atom. However, these sequential H loss mechanisms lie very high in energy when compared to the mechanism seen in Figure 2.

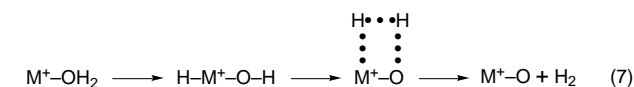
The observed reaction leading to  $\text{HTi}^+(^3\Delta) + \text{OH}$  is also possible from the  $\text{HTi}^+\text{OH}$  quartet intermediate. A simple breaking of the Ti–O bond leads to these energetically high-lying products. A similar process on the doublet surface, leading to singlet  $\text{TiH}^+ + \text{OH}$ , is even more energetically disfavored with a final energy 0.891 eV higher than that of triplet  $\text{TiH}^+ + \text{OH}$ . Thus it lies outside of the energy range depicted in Figure 3.

Equilibrium geometry parameters for the various reaction products are given in Figure 6.

**3.7. The  $\text{H}_2$  Elimination Mechanism.** There has been much discussion in the literature as to what is the process of  $\text{H}_2$  elimination induced by transition metal ions.<sup>10,11,13</sup> The two leading contenders have the following schemes:



and



Our theoretical results imply that neither of these is entirely correct, nor are they entirely in error.

Our predictions agree with mechanism 6 in so much as the hydrogen atoms are last associated with  $\text{Ti}^+$  before elimination. However, a quick examination of the bonding shows that there are not two Ti–H covalent bonds; rather this species should be considered an ion–molecule complex. There is  $d \rightarrow \sigma^*$  donation that activates the H–H bond, but the H–H bond is intact and no covalent Ti–H bond exists.

Mechanism 7 is incorrect, according to our predictions, *only* in that the four-centered transition state is shown leading directly to  $\text{MO}^+ + \text{H}_2$ . We predict the existence of another intermediate,  $(\text{H}_2)\text{TiO}^+$ , through which the reaction passes.

In examining the two intermediates,  $\text{HTi}^+\text{OH}$  and  $(\text{H}_2)\text{TiO}^+$ , it is seen that the connection between the two *must* be a four-centered transition state. From the  $\text{HTi}^+\text{OH}$  intermediate a second hydrogen transfer to  $\text{Ti}^+$  does not occur; rather a hydrogen transfer to hydrogen is seen. This process is multifaceted. It involves the breaking of the O–H bond, the forming of the H–H bond, the breaking of one covalent Ti–H bond, and the formation of a Ti–O  $\pi$  bond.

Armentrout and co-workers<sup>11</sup> suggest that for the four-centered transition state  $\text{TiO}_{(3\pi)} \rightarrow \text{H}-\text{H}_{(\sigma^*)}$  donation is important. This implies a planar four-center transition state. Indeed we find that there is significant interaction between the  $\text{TiO} \pi$  system and the H–H bond being formed. Figure 7 depicts

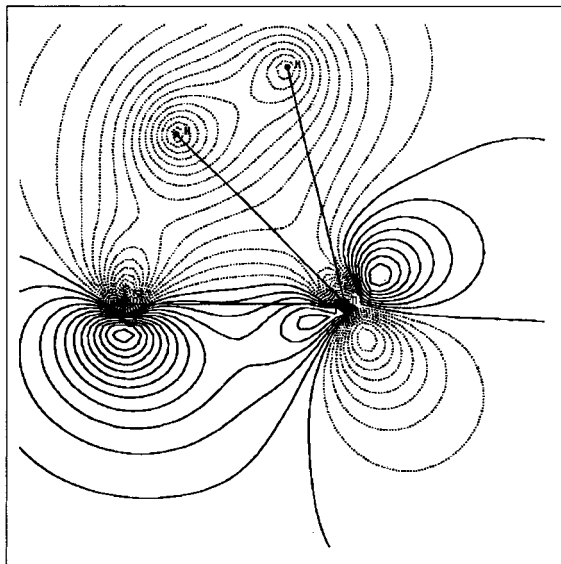


**Figure 7.**  $\sigma_{\text{H-H}} + \pi_{\text{TiO}}$  molecular orbital of the doublet four-centered transition state.

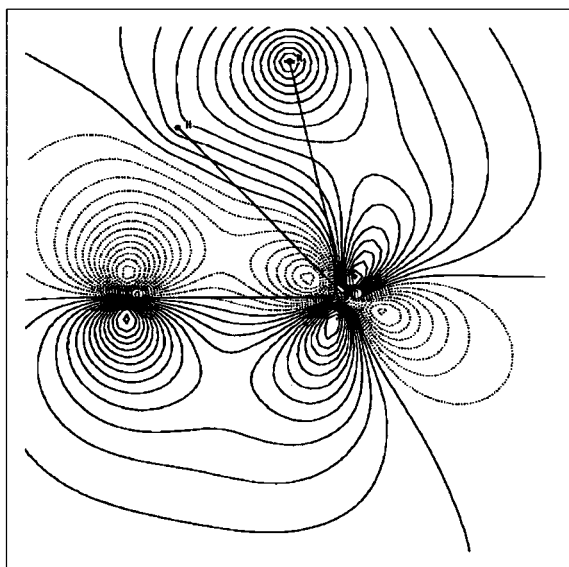


**Figure 8.**  $\sigma_{\text{H-H}} - \pi_{\text{TiO}}$  molecular orbital of the doublet four-centered transition state.

the  $\sigma_{\text{H-H}} + \pi_{\text{TiO}}$  orbital with large positive overlap for all the atoms. Figure 8 illustrates that the  $\sigma_{\text{H-H}} - \pi_{\text{TiO}}$  orbital is stabilized by positive overlap with one lobe of the in-plane d orbital on Ti. Figure 9 shows the singly occupied orbital of this doublet. The interaction here is  $\pi_{\text{TiO}}^* + \sigma_{\text{H-H}}^*$ .

Planar transition states for  $\text{H}_2$  rotation also were found for both the doublet and quartet  $(\text{H}_2)\text{TiO}^+$  species, lying only 0.004 and 0.026 eV above their respective minima. We suggest that these low-lying transition states could be related to the four-centered transition state.

Thus our results support the hypothesis of a four-centered transition state that leads eventually to  $\text{H}_2$  elimination. The difference between our predictions and that original hypothesis is that we have found another intermediate  $(\text{H}_2)\text{TiO}^+$  through which the reaction passes.

Another possible reaction path, originally discussed by Irikura and Beauchamp in studying  $\text{OsO}_x^+(x = 1-4) + \text{H}_2$ ,<sup>37</sup> involves direct separation of  $\text{H}_2$  from the O atom of the  $\text{Ti}(\text{OH}_2)^+$  structure without any hydrogen transfer to titanium (or in the reverse reaction  $\text{H}_2$  attaching directly to the oxygen atom of

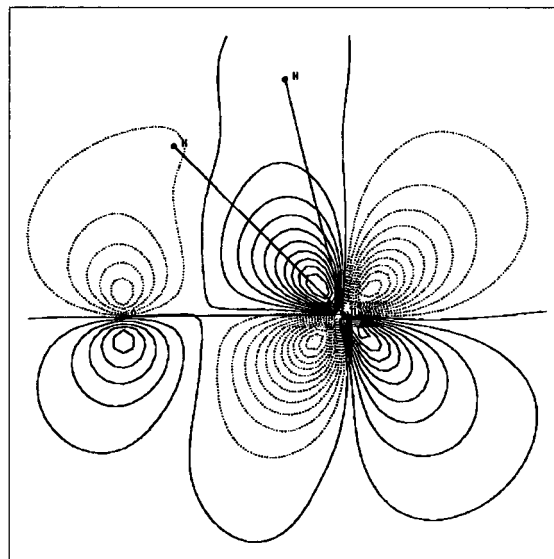


**Figure 9.** Singly occupied  $\pi_{\text{TiO}} + \sigma_{\text{H-H}}$  molecular orbital of the doublet four-centered transition state.

$\text{Ti-O}^+$ ). Transition states corresponding to the direct loss of a hydrogen molecule from the initial  $\text{Ti}(\text{OH}_2)^+$  ion-molecule on both surfaces were sought. However, the imaginary frequencies of the  $\text{Ti-O}^+\cdots\text{H}_2$  stationary points located were indicative of sequential H loss, rather than loss of  $\text{H}_2$ . Thus, this proposed reaction mechanism is ruled out in this case.

#### 4. Conclusions

The reaction of  $\text{Ti}^+$  with water has been investigated in detail. Both the doublet and quartet potential energy surfaces have been characterized at the B3LYP/DZVP level of theory. Energy differences between key doublet and quartet species and total reaction energies for the experimentally observed products have been predicted at even higher levels of theory including B3LYP/TZVP+G(3df,2p) and CASPT2/Wachters. From these data, the following conclusions are drawn:

- (1) The only exothermic products of the  $\text{Ti}^+(^4\text{F},^2\text{F}) + \text{H}_2\text{O}$  reaction are  $\text{TiO}^+(^2\Delta) + \text{H}_2$ .
- (2) The  $\text{HTi}^+\text{OH}$  intermediate hypothesized by the experimentalists is a well-defined minimum on each potential energy surface.
- (3) The doublet and quartet potential energy surfaces cross between this aforementioned intermediate and the  $\text{Ti}(\text{OH}_2)^+$  ion-molecule complex.
- (4) The much-discussed  $\text{H}_2$  elimination process occurs neither from a  $\text{H}_2\text{TiO}^+$  species with two covalent  $\text{Ti-H}$  bonds nor directly from a four-centered transition state, but rather passes from the  $\text{HTi}^+\text{OH}$  intermediate through a four-centered transition state to another ion-molecule intermediate  $(\text{H}_2)\text{TiO}^+$ , from which intermediate  $\text{H}_2$  is eliminated.

**Acknowledgment.** This research has been supported by a grant (UPV/203.215-EB247/95) from The University of the Basque Country (Euskal Herriko Unibertsitatea). We are also indebted to a referee who provided insightful, well-thought-out commentary on our original manuscript. J.E.F. and A.I. thank the Basque Government for a Grant. A.I. also thanks Prof. L. A. Eriksson, in particular, and all the Quantum Chemistry group of the University of Stockholm, in general, for helpful comments and great hospitality.

## References and Notes

- (1) Siegbahn, P. E. M. Electronic structure calculations for molecules containing transition metals. *Adv. Chem. Phys.* **1996**, *XCIII*, 333–386.
- (2) Gordons, M. S.; Cundari, T. R. *Coord. Chem. Rev.* **1996**, *147*, 87.
- (3) Martinho-Simoes, J. A.; Beauchamp, J. L. *Chem. Rev.* **1990**, *90*, 629–688.
- (4) Dalleska, N. F.; Honma, K.; Sunderlin, L. S. Armentrout, P. B. *J. Am. Chem. Soc.* **1994**, *116*, 3519.
- (5) Clemmer, D. E.; Chen, Y.-M.; Aristov, N.; Armentrout, P. B. *J. Phys. Chem.* **1994**, *98*, 7538.
- (6) Magnera, T. F.; David, D. E.; Michl, J. *J. Am. Chem. Soc.* **1989**, *111*, 4100.
- (7) Chen Y.-M., Clemmer, D. E.; Armentrout, P. B. *J. Am. Chem. Soc.* **1994**, *116*, 7815
- (8) Clemmer, D. E.; Sunderlin, L. S.; Armentrout, P. B. *J. Phys. Chem.* **1990**, *94*, 3008.
- (9) Kickel, B. L.; Armentrout, P. B. *J. Am. Chem. Soc.* **1994**, *116*, 10742.
- (10) Guo, B. C.; Kerns, K. P.; Castleman, A. W. *J. Phys. Chem.* **1992**, *96*, 4879–4883.
- (11) Clemmer, D. E.; Aristov, N.; Armentrout, P. B. *J. Phys. Chem.* **1993**, *97*, 544–552.
- (12) Tilson, J. L.; Harrison, J. F. *J. Phys. Chem.* **1991**, *95*, 5097.
- (13) Chen, Y. M.; Clemmer, D. E.; Armentrout, P. B. *J. Phys. Chem.* **1994**, *98*, 11490–11498.
- (14) Irigoras, A.; Ugalde, J. M.; Lopez, X.; Sarasola, C. *Can. J. Chem.* **1996**, *74*, 1824–1829.
- (15) Becke, A. D. *Phys. Rev. A* **1988**, *38*, 3098.
- (16) Lee, C.; Yang, W.; Parr, R. G. *Phys. Rev. B* **1988**, *37*, 785.
- (17) Sim, F.; Salahub, D. R.; Chim, S.; Dupuis, M. *J. Chem. Phys.* **1991**, *95*, 4317.
- (18) Godbout, N.; Salahub, D. R.; Andzelm, J.; Wimmer, E. *Can. J. Chem.* **1992**, *70*, 560.
- (19) Ricca, A.; Bauschlicher, C. W. *J. Phys. Chem.* **1994**, *98*, 12899.
- (20) Bauschlicher, C. W.; Maitre, P. *J. Phys. Chem.* **1995**, *99*, 3444.
- (21) Schäfer, A.; Hurbert, C.; Ahlrichs, R. *J. Chem. Phys.* **1994**, *100*, 5829.
- (22) Wachters, A. J. *J. Chem. Phys.* **1970**, *52*, 1033.
- (23) Hay, P. J. *J. Chem. Phys.* **1971**, *66*, 4377.
- (24) Raghavachari, K.; Trucks, G. W. *J. Chem. Phys.* **1989**, *91*, 1062.
- (25) Krishnan, J. S.; Binkley, J. S.; Seeger, P. v. R.; Pople, J. A. *J. Chem. Phys.* **1980**, *72*, 650.
- (26) Andersson, K.; Malmqvist, P.-Å.; Roos, B. O.; Sadlej, A. J.; Wolinski, K. *J. Phys. Chem.* **1990**, *94*, 5483.
- (27) Andersson, K.; Malmqvist, P.-Å.; Roos, B. O. *J. Chem. Phys.* **1992**, *96*, 1218.
- (28) Blomberg, M. R. A.; Siegbahn, P. E. M.; Svensson, M. *J. Chem. Phys.* **1996**, *104* (23), 9546.
- (29) Huzinaga, S. *J. Chem. Phys.* **1965**, *42*, 1293.
- (30) Musaev, D.G.; Morokuma, K. *J. Phys. Chem.* **1996**, *100*, 11600.
- (31) Frish, M. J.; Trucks, G. W.; Schlegel, H. B.; Gill, P. M. W.; Johnson, B. G.; Robb, M. A.; Cheeseman, J. R.; Keith, T. A.; Petersson, G. A.; Montgomery, J. A.; Raghavachari, K.; Al-Laham, M. A.; Zakrzewski, V. G.; Ortiz, J. V.; Foresman, J. B.; Cioslowski, J.; Stefanov, B. B.; Nanayakkara, A.; Challacombe, M.; Peng, C. Y.; Ayala, P. Y.; Chen, W.; Wong, M. W.; Andres, J. L.; Replogle, E. S.; Gomperts, R.; Martin, R. L.; Fox, D. J.; Binkley, J. S.; Defrees, D. J.; Baker, J.; Stewart, J. P.; Head-Gordon, M.; Gonzalez, C.; Pople, J. A. *Gaussian 94* (Revision A.1); Gaussian, Inc.: Pittsburgh, PA, 1995.
- (32) Andersson, K.; Füscher, M. P.; Karlström, G.; Lindh, R.; Malmqvist, P.-Å.; Olsen, J.; Roos, B. O.; Sadlej, A. J.; Blomberg, M. R. A.; Siegbahn, P. E. M.; Kellö, V.; Noga, J.; Urban, M.; and Widmark, P.-O. MOLCAS Version 3; Dept. of Theor. Chem., Chem. Center, Univ. Of Lund, P.O. Box 124, S-221 00 Lund, Sweden, 1994.
- (33) Read, A. E.; Curtiss, L. A.; Weinhold, v. F. *Chem. Rev.* **1988**, *88*, 899.
- (34) NBO Version 3.1, Glendening, A. E.; Read, A. E.; Carpenter, J. E.; Weinhold, v. F.
- (35) MOLDEN, a visualization program of molecular and electronic structure. <http://www.caos.kun.nl/~schaft/molden/molden.html>.
- (36) Rosi, M.; Bauschlicher, C. W. *J. Chem. Phys.* **1989**, *90* (12), 7264.
- (37) Irikura, K. K.; Beauchamp, J. L. *J. Am. Chem. Soc.* **1989**, *111*, 75.
- (38) Moore, C. E. *Atomic Energy Levels*; National Bureau of Standards: Washington, DC, 1952; *Natl. Bur. Stand. Circ.* **1959**, *2* (3), 467.